過去三年中(2008 年 8 月至 2011 年 7 月)，本實驗室在國科會經費支持下對鐵-(20~25) at.%鋁-(6~9) at.%鈦合金的相變化進行研究，並已將其中部分研究成果整理成論文發表，其餘研究成果也正在整理準備發表中。較重要的成果為：(1) 在鐵-20 at.%鋁-8 at.%鈦合金中，發現鐵-20 at.%鋁-8 at.%鈦合金的淬火顯微結構為(A2＋$D0_3$)，當此合金在 1000˚C 時效處理時，C14 相將會 A2 基地中析出，且 C14 與 A2 基地的晶體關係為$(0\,0\,0\,1)_{C14}//(\bar{1}\,\bar{1}\,2)_m$, $(\bar{1}\,1\,0\,0)_{C14}//(\bar{1}\,1\,0)_m$, $(1\,1\,\bar{2}\,0)_{C14}//(1\,1\,1)_m$。這部分的結果我們已整理成論文" Orientation relationship between C14 precipitate and ferrite matrix in an Fe-20Al-8Ti alloy "發表於期刊 Scripta Materialia。(2) 我們發現在淬火狀態下，鐵-23 at.%鋁-8.5 at.%鈦合金的淬火顯微結構為(A2＋$D0_3$)。當此合金在 900℃時效處理時，$D0_3$ 大小會隨者時效時間的增加而變大，且在 a/2<100>反相界面(APBs)中發生了 A2 →B2→(A2+$D0_3$) 規律化變態，此現象從未在其它之 Fe-Al-Ti 合金系統研究中發現。這部分的結果我們已整理成論文" Formation of (B2+D03) phases at a/2<100> anti-phase boundary in an Fe-23 at.% Al-8.5 at.% Ti alloy"發表於期刊 Scripta Materialia。(3) 在淬火狀態下，鐵-23 at.%鋁-7 at.%鈦合金的淬火顯微結構為(A2＋$D0_3$)，此顯微結構為淬火過程中合金經由 A2 →B2→(A2+$D0_3$) 規律化變態所產生的。當此合金於 800℃時效處理時，$D0_3$ 區域會以<100>方向成長，且具有極細微之 B2 顆粒在 a/2<100>反相界面上。在經更長時間時效處理時，細微之 B2 顆粒將會取代了整個 a/2<100>反相界面。因此，此合金在 800℃時的穩定結構為(B2+$D0_3$)。這部分的結果我們已整理成論文" Formation of (B2+D03) two-phase microstructure in a Fe-23 Al-7 Ti alloy "發表於期刊 Mater. Trans.。(4) 在鐵-24.6 at.%鋁-7.5 at.%鈦合金中，發現鐵-24.6 at.%鋁-7.5 at.%鈦合金的淬火顯微結構為(A2＋$L2_1$)，其乃在淬火過程中經由 A2 →B2→(A2+ $L2_1$) 規律化變態所形成的。當此合金在 900˚C 適當時間之時效處理後，發現 $L2_1$ 區域成長，並且由於原本的 $L2_1$ 區域成長時鈦及鋁原子會往 a/2<100>反相晶界擴散促使 A2 →B2 反應發生在 a/2<100>反相晶界上，故 B2 相會開始沿著 a/2<100>反相晶界析出。隨著時效時間的增加，$L2_1$ → (B2+ $L2_1$*)相分離(phase separation)的現象會在 a/2<100>反相晶界處開始發生，並且持續相分離到先前完整的 $L2_1$ 區域。由於 $L2_1$*中的鈦含量明顯較原本的 $L2_1$ 高而鋁含量稍低，而在鐵-鋁合金中 $L2_1$ 相僅在鋁含量＞25 at.%、溫度低於 550℃時才存在，故此現象也說明了鈦對 $L2_1$ 在高溫時的穩定有很重要的作用。此種 $L2_1$ → (B2+ $L2_1$*)相分離的微觀結構變化至今從未被其他學者在鐵-鋁-鈦合金系統中發現過。這部分的結果我們已整理成論文"Phase separation from $L2_1$ to (B2+ $L2_1$) in an Fe-24.6Al-7.5Ti alloy"發表於期刊 Mater. Trans.。接下來除舉出我們已投稿論文外，另列出本研究群正執行中之數項技術轉移案、及已獲通過或正申請中的專利，本篇報告內容則為本研究群對鐵-(20~25) at.%鋁-(7~9) at.%鈦合金之研究成果。

一、論文：

1. 期刊名稱：Mater. Trans.
   計畫編號：NSC97-2221-E009-027-MY3
   著作內容：G.D. Tsay, C.W. Su, Y.H. Tuan, C.G. Chao and T.F. Liu, "Phase separation from L21 to (B2+L21) in Fe-24.6Al-7.5Ti alloy", Mater. Trans. Vol. 51, No. 10, pp. 1934-1938.
2. 期刊名稱：Mater. Trans.
   計畫編號：NSC97-2221-E009-027-MY3
   著作內容：C.W. Su, C.G. Chao and T.F. Liu, "Formation of (B2+$D0_3$) Two-Phase Microstructure in a Fe-23Al-7Ti Alloy", Vol. 48, No. 11, pp. 2993-2996.
3. 期刊名稱：Scripta Mater.

計畫編號：NSC97-2221-E009-027-MY3

著作內容：C.W. Su, C.G. Chao and T.F. Liu, "Formation of (B2+$D0_3$) Phases at a/2<100> Anti-Phase Boundary in an Fe-23 at.% Al-8.5 at.% Ti Alloy", Vol. 57, pp. 917-920.

4. 期刊名稱：Scripta Mater.

計畫編號：NSC97-2221-E009-027-MY3

著作內容：C.W. Su, S.C. Jeng, C.G. Chao and T.F. Liu, "Orientation Relationship between C14 Precipitate and Ferrite Matrix in an Fe-20 at.% Al-8 at.% Ti Alloy", Vol. 57, pp. 125-128.

二、技術轉移案：

(1) 鐵鋁錳碳合金高爾夫球頭精密鑄造、鍛造和鑄鍛系列產品（復盛、明安、鉅明等三家公司，2005~2010）

(2) 刀削式鰭片散熱器、刀具及其加工法（聚亨公司，2003~2009）

三、專利：

(1) 低密度高強度高韌性合金材料及其製法（High Strength and High Toughness Alloy with Low Density and The Method of Making）（2007~2025，中華民國專利 I279448 號、美國專利 20070084528 公告中、日本專利正在審核中）

(2) 刀削式鰭片散熱器、刀具及其加工法（2003~2018，中華民國專利 511449 號）

(3) 低密度高韌性合金材料及其製法（Low Density And High Toughness Alloy And The Process For Making Same）（中華民國、美國、日本專利申請中）

(4) 低密度合金材料及其製法（Low Density Alloy And The Method of Making）（中華民國、美國、日本專利申請中）

Orientation relationship between C14 precipitate and ferrite matrix in an Fe-20Al-8Ti alloy

＊C.W. Su*、Chih-Lung Lin、Kai-Ming Chang、Po-Chih Chen、Yung-Chang Chen、Cheng-Yi Lin、C.G. Chao、T.F. Liu

Department of Materials Science and Engineering,National Chiao Tung University,

（NSC 97-2221-E-009-027-MY3）

Abstract

C14 precipitates were observed to appear within the ferrite matrix in the Fe-20Al-8Ti alloy aged at 1000℃. By means of transmission electron microscopy and diffraction techniques, the orientation relationship between the C14 precipitate and ferrite matrix was determined as follows: $(0\,0\,0\,1)_{C14}//(\bar{1}\,\bar{1}\,2)_m$, $(\bar{1}\,1\,0\,0)_{C14}//(\bar{1}\,1\,0)_m$, $(1\,1\,\bar{2}\,0)_{C14}//(1\,1\,1)_m$. The present result of the orientation relationship between the two phases has never been reported by previous workers in the Fe-Al-Ti alloy systems before

Keywords：Fe-Al-Ti alloy; C14 phase; Orientation relationship

Introduction

The microstructures of the Fe-Al-Ti alloys have been studied by other workers [1-6]. In their studies, it is seen that only four phase fields, namely α(ferrite), α+D03, D03 and B2, could be found in the Fe-(18~25) at.% Al-Ti alloys with Ti≦5 at.% [1,2]. However, when the Ti content was increased to 7 at.% or above, C14 precipitates could be investigated to form within the B2 or α matrix in the aged Fe-Al-Ti alloys [2-6]. The C14 precipitate has a hexagonal structure with lattice parameters a=0.5038 nm and c=0.8193 nm [6]. Although the C14 precipitate was extensively reported to be detected in the aged Fe-Al-Ti alloys, little information concerning the orientation relationship between the C14 precipitate and matrix has been provided. Therefore, the purpose of the present study is an attempt to determine the orientation relationship between the C14 precipitate and α matrix in the Fe-20Al-8Ti alloy.

Experimental Procedure

The Fe-20 at.%Al-8 at.%Ti alloy was prepared in a vacuum induction furnace by using 99.5% Fe, 99.9% Al and 99.7% Ti. The melt was chill cast into a 30 × 50 × 200-mm-copper mold. After being homogenized at 1250 ℃ for 48h, the ingot was sectioned into 2-mm-thick slices. These slices were subsequently solution heat-treated at 1250℃ for 2h and then quenched into room-temperature water rapidly. The aging processes were performed at 1000℃ for various times in a vacuum heat-treated furnace and then quenched rapidly. TEM specimens were prepared by means of double-jet electropolisher with an electrolyte of 67% methanol and 33% nitric acid. The polishing temperature was kept in the range from -30℃ to -20℃, and the current density was kept in the range from 4.0×10^4 to 6.0×10^4 A/m^2. Electron microscopy was performed on a JEOL JEM-2000FX scanning transmission electron microscope operating at 200KV

Results and Discussion

Figure 1(a) is a bright-field (BF) electron micrograph of the as-quenched alloy. Figure 1(b) is a selected-area diffraction pattern (SADP) of the as-quenched alloy, exhibiting the superlattice reflection spots of the ordered $D0_3$ phase [7]. Figure 1(c) is a $(1\bar{1}1)$ $D0_3$ dark-field (DF) electron micrograph of the as-quenched alloy, revealing the presence of extremely fine $D0_3$ domains. Figure 1(d), a (002) DF electron micrograph, shows the presence of small B2 domains and a high density of disordered α phase (dark contrast) within the B2 domains. Since the sizes of both $D0_3$ and B2 domains are very small, it is deduced that the (α+$D0_3$) phases existing in the as-quenched alloy were formed by a α→B2→(α+$D0_3$) ordering transition during quenching. This result is similar to that observed by other workers in the Fe-(18~22.5) at.% Al-5 at.% Ti alloys [1]

When the as-quenched alloy was aged at 1000℃ for moderate times, some plate-like precipitates started to appear within the matrix. A typical example is shown in Figure 2(a). Figures 2(b) and (c) are the $(1\bar{1}1)$ and (002) $D0_3$ DF electron micrographs taken from the same area as Figure 2(a), indicating the existence of the small quenched-in $D0_3$ and B2 domains, respectively. Figures 2(d) through (f) show three different SADPs taken from the plate-like precipitate marked as “C” in Figure 2(a). According to the camera length and the measurement of d-spacings as well as angles among the reciprocal lattice vectors of the diffraction spots, the crystal structure of the precipitate was determined to be hexagonal with lattice parameters a=0.505 nm and c=0.817 nm, which corresponds to that of the C14 phase [6]. The zone axes of the precipitate in Figures 2(d) through (f) are $[0\,0\,0\,1]$, $[1\,1\,\bar{2}\,0]$ and $[1\,1\,\bar{2}\,\bar{3}]$, respectively. Based on the above examinations, it is concluded that the microstructure of the alloy present at 1000℃ should be a mixture of (α+C14) phases.

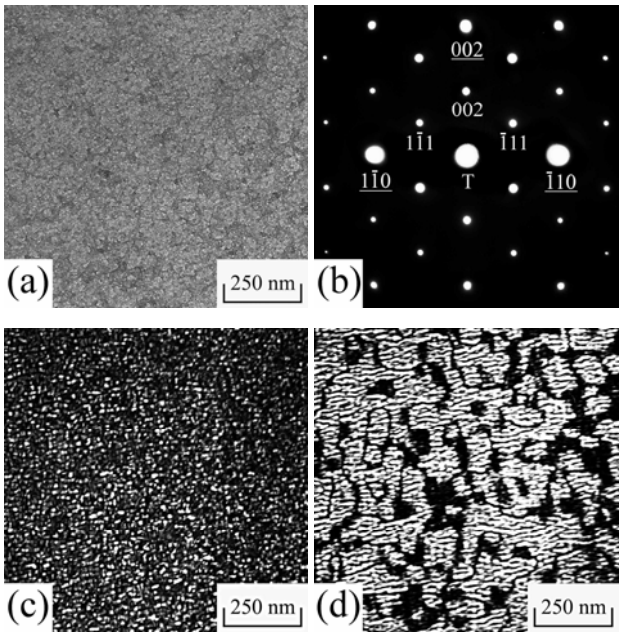

Figure 1. Electron micrographs of the as-quenched alloy: (a) BF, (b) an SADP. The foil normal is [1 1 0]. (hkl = ferrite phase; hkl = $D0_3$ phase.), (c) and (d) (1 $\bar{1}$1) and (002) $D0_3$ DF, respectively.

In order to determine the orientation relationship between the C14 precipitate and the (α+$D0_3$) matrix, ten different SADPs were taken from an area including the precipitate marked as "C" in Figure 2(a) and its surrounding (α+$D0_3$) phases. The results are shown in Figures 3(a) through (j). These SADPs were obtained by tilting the specimen about some specific reflections. The zone axes of the C14 precipitate and (α+$D0_3$) matrix in Figures 3(a) through (j) are [1 1 $\bar{2}$ 0]$_{C14}$, [1 1 1]$_m$; [2 2 $\bar{4}$ 3]$_{C14}$, [1 1 0]$_m$; [5 5 $\bar{10}$ $\bar{12}$]$_{C14}$, [$\bar{3}$ $\bar{3}$ 1]$_m$; [1 1 $\bar{2}$ $\bar{3}$]$_{C14}$, [$\bar{2}$ $\bar{2}$ 1]$_m$; [1 1 $\bar{2}$ $\bar{6}$]$_{C14}$, [$\bar{1}$ $\bar{1}$ 1]$_m$; [0 0 0 1]$_{C14}$, [$\bar{1}$ $\bar{1}$ 2]$_m$; [7 1 $\bar{8}$ $\bar{6}$]$_{C14}$, [2 1 0]$_m$; [13 5 $\bar{8}$ $\bar{6}$]$_{C14}$, [1 0 0]$_m$; [7 $\bar{2}$ $\bar{5}$ $\bar{6}$]$_{C14}$, [$\bar{5}$ $\bar{1}$ 1]$_m$ and [5 $\bar{1}$ $\bar{4}$ $\bar{6}$]$_{C14}$, [$\bar{3}$ $\bar{1}$ 1]$_m$, respectively. For better demonstration, higher magnification of Figures 3(a), (b), (f) and (h) is shown in Figures 4(a) through (d), respectively. It is obvious in Figures 4(a) and (c) that the (0 0 0 1) and (1 1 $\bar{2}$ 0) reflection spots of the C14 precipitate are nearly parallel to the ($\bar{1}$ $\bar{1}$ 2) and (1 1 1)interplanar angles between the chosen reciprocal reflections of the C14 precipitate were obtained by calculation using the following equation [8]:reflection spots of the matrix, respectively. By means of this information, a stereographic plot of poles (superimposing the (0 0 0 1) projection of the C14 precipitate and the ($\bar{1}$ $\bar{1}$ 2) projection of the matrix) was constructed, as shown in Figure 5, where the (1 1 $\bar{2}$ 0) pole of the C14 precipitate was made to match with the (1 1 1) pole of the α matrix. In this stereographic plot, the interplanar angles between the chosen reciprocal reflections of the C14 precipitate were obtained by calculation using the following equation [8]:

$$\cos\phi = \frac{h_1h_2 + k_1k_2 + \frac{1}{2}(h_1k_2 + k_1h_2) + \frac{3a^2}{4c^2}l_1l_2}{\left\{\left(h_1^2 + k_1^2 + h_1k_1 + \frac{3a^2}{4c^2}l_1^2\right)\left(h_2^2 + k_2^2 + h_2k_2 + \frac{3a^2}{4c^2}l_2^2\right)\right\}^{\frac{1}{2}}}$$

It is clear in Figure 5 that the ($\bar{1}$ 1 0 0), (1 1 $\bar{2}$ 4), (1 1 $\bar{2}$ 1) *et al.* poles of the C14 precipitate would exactly or nearly coincide with the ($\bar{1}$ 1 0), (0 0 1), (1 1 2) *et al.* poles of the matrix. These results are quite consistent with the observations of SADPs in Figures 3 and 4. On the basis of the preceding analyses, the orientation relationship between the C14 precipitate and α matrix can be best stated as follows: (0 0 0 1)$_{C14}$//($\bar{1}$ $\bar{1}$ 2)$_m$, ($\bar{1}$ 1 0 0)$_{C14}$//($\bar{1}$ 1 0)$_m$, (1 1 $\bar{2}$ 0)$_{C14}$//(1 1 1)$_m$

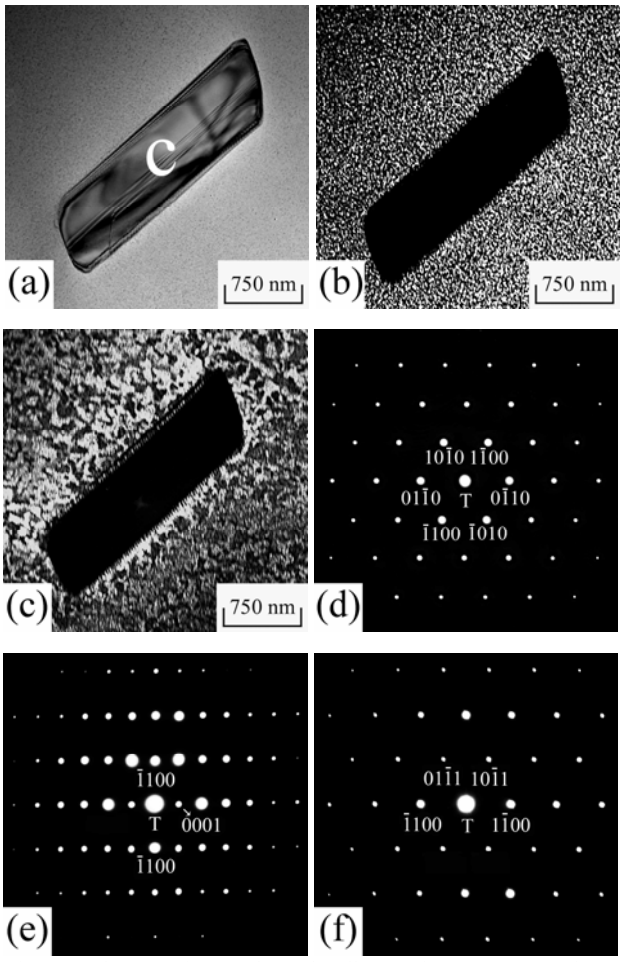

Figure 2. Electron micrographs of the alloy aged at 1000°C for 1 h: (a) BF, (b) and (c) (1 $\bar{1}$1) and (002) $D0_3$ DF, respectively. , (d) through (f) three SADPs taken from the precipitate marked as "C" in Figure 2(a). The zone axes of the C14 precipitate are (d) [0 0 0 1], (e) [1 1 $\bar{2}$ 0] and (f) [1 1 $\bar{2}$ $\bar{3}$], respectively.

Finally, it is worthwhile to mention that the C14 precipitate was also observed by many workers in Fe-Al-Nb, Fe-Al-Zr and Fe-Al-Ta alloys [4, 9-10]. However, we are aware of only one article, in which the orientation relationship between the C14 precipitate and α matrix was predicted. In 2005, Morris et al. reported that when the Fe-25Al-2Nb alloy was aged at 800℃ or 900℃, C14 precipitate were formed within the α matrix; the orientation relationship between the C14 precipitates and α matrix was $\{\bar{1}010\}_{C14}//\{\bar{1}01\}_m$, $<1\bar{2}10>_{C14} \approx <010>_m$ and $<0001>_{C14} \approx <101>_m$, which was determined by using two SADPs [9]. Interestingly, it is noted here that the previous result of $\{\bar{1}010\}_{C14}//\{\bar{1}01\}_m$ is indeed in agreement with that observed in Figure 4(c) of the present work.

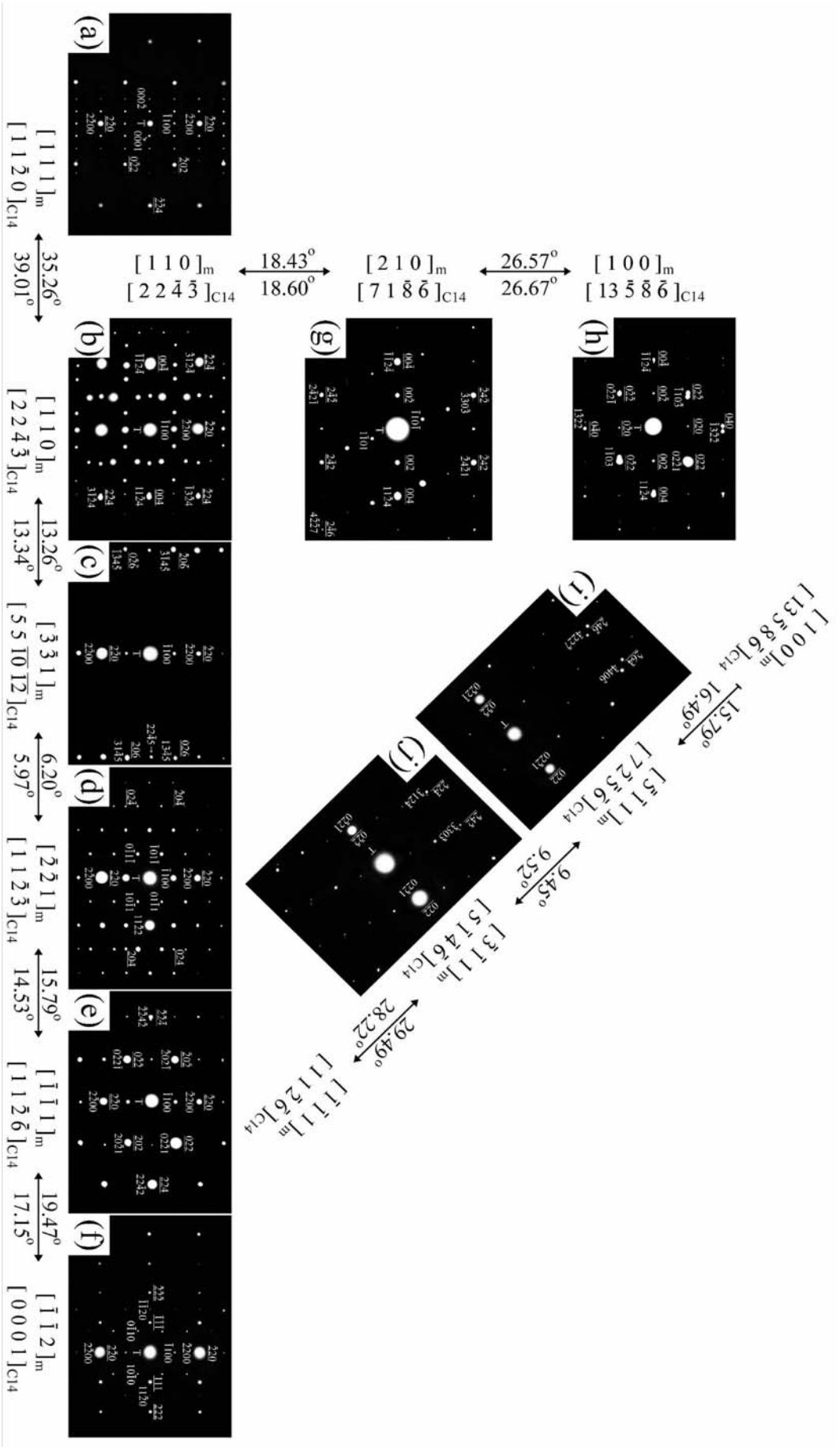

Figure 3. Ten SADPs taken from an area including the precipitate marked as "C" in Fig. 2(a) and its surrounding matrix. The zone axes of the matrix are (a)[1 1 1], (b)[1 1 0], (c)[$\bar{3}$ $\bar{3}$ 1], (d)[$\bar{2}$ $\bar{2}$ 1], (e) [$\bar{1}$ $\bar{1}$ 1], (f)[$\bar{1}$ $\bar{1}$ 2], (g)[2 1 0], (h)[1 0 0], (i) [$\bar{5}$ $\bar{1}$ 1] and (j) [$\bar{3}$ $\bar{1}$ 1], respectively (hkil = C14 phase; hkl = matrix).

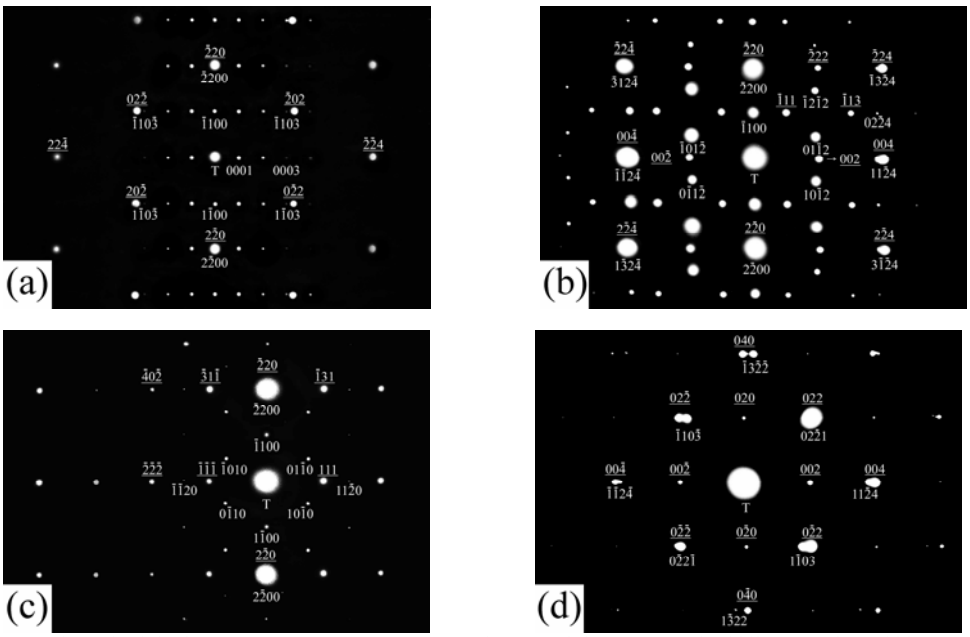

Figure 4. (a) through (d) higher magnification of Figures 3(a), (b), (f) and (h), respectively (hkil = C14 phase; hkl = matrix).

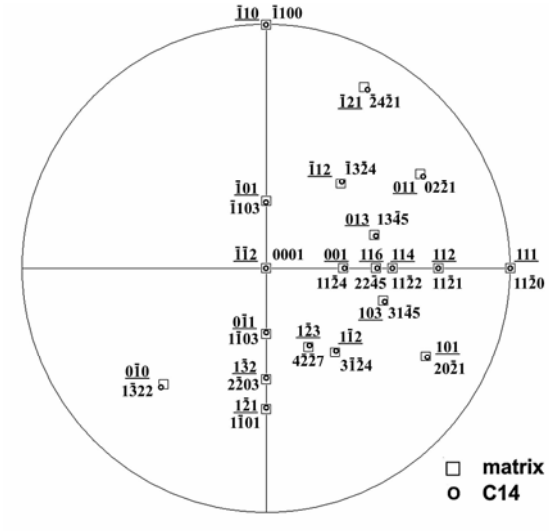

Figure 5. The superimposed C14/ferrite stereogram describing the orientation relationship between the C14 precipitate and ferrite matrix.

Conclusion

The as-quenched microstructure of the Fe-20 at.%Al-8 at.%Ti alloy was a mixture of (α+$D0_3$) phases. When the alloy was aged at 1000℃, C14 precipitates were observed to occur within the α matrix. The orientation relationship between the C14 precipitate and α matrix can be best stated as follows:
$(0001)_{C14}//(\bar{1}\bar{1}2)_m$, $(\bar{1}100)_{C14}//(\bar{1}10)_m$, $(11\bar{2}0)_{C14}//(111)_m$.

Acknowledgements

The authors are pleased to acknowledge the financial support of this research by the National Science Council, Republic of China under Grant NSC 97-2221-E-009-027-MY3.

References

[1] M.G. Mediratta, S.K. Ehlers, H.A. Lipsitt, Metall. Trans. A 18 (1987) 509.
[2] C.H. Sellers, T.A. Hyde, T.K. O'Brien, R.N. Wright, J. Phys. Chem. Solids 55 (1994) 505.
[3] U. Prakash, G. Sauthoff, Intermetallics 9 (2001) 107.
[4] M. Palm, Intermetallics 13 (2005) 1286.
[5] M. Palm, G. Sauthoff, Intermetallics 12 (2004) 1345.
[6] M. Palm, G. Inden, N. Thomas, J. Phase Equilibria 16 (1995) 209.
[7] C.H. Chen, T.F. Liu, Metall. Trans. A 34 (2003) 503.
[8] J. W. Edington, The Operation and Calibration of the Electron Microscope, Vol.1, (1985).
[9] D.G. Morris, L.M. Requejo, M.A. Muñoz-Morris, Intermetallics 13 (2005) 862.
[10] F. Stein, M. Palm, G. Sauthoff, Intermetallics 13 (2005) 1056.
[11] F. Stein, M. Palm, G. Sauthoff, Intermetallics 13 (2005) 1275.

Formation of ($B2+D0_3$) phases at a/2<100> anti-phase boundary in an Fe-23 at.% Al-8.5 at.% Ti alloy

Chun-Wei Su, Chih-Lung Lin, Kai-Ming Chang, Po-Chih Chen, Yung-Chang Chen, Cheng-Yi Lin, C.G. Chao and T.F. Liu*

Department of Materials Science and Engineering, National Chiao Tung University,

（NSC 97-2221-E-009-027-MY3）

Abstract

The as-quenched microstructure of the Fe-23 at.% Al-8.5 at.% Ti alloy was a mixture of ($A2+D0_3$) phases. Transmission electron microscopy (TEM) examinations indicated that when the alloy was aged at 900° C, the size of the $D0_3$ domains increased with increasing aging time, and an A2 → ($A2+D0_3$) → ($B2+D0_3$) transition occurred at a/2<100> anti-phase boundaries (APBs). This feature has never been reported by other workers in the Fe-Al-Ti alloy systems before.

Keywords: iron alloys; phase transformations; TEM; anti-phase boundary.

Introduction

In order to improve high temperature oxidation and mechanical properties, Ti has been added to the Fe-Al binary alloys [1-5]. Based on these results, it can be generally concluded that the addition of Ti can effectively improve these properties. In addition, the effects of Ti addition on the microstructures of the Fe-Al binary alloys have also been studied by many workers [3-13]. It was reported that the addition of Ti would strongly increase the $D0_3$→B2 and B2→ A2 transition temperatures [6-13], and expand the ($A2+D0_3$) phase field [10-12]. Furthermore, a ($B2+D0_3$) two-phase field was claimed to be existent in the Fe-Al-Ti ternary alloys [11-13]. It is worthwhile to note that the ($B2+D0_3$) two-phase field has not been found by previous workers in the Fe-Al binary alloys before [14-16]. However, to date, the existence of the ($B2+D0_3$) two-phase field in the Fe-Al-Ti ternary alloys was confirmed principally by using X-ray diffraction and electron-probe microanalysis [11-13]. In order to clarify the microstructural revolution for the formation of the ($B2+D0_3$) phases, a TEM study was performed to investigate the phase transition in the Fe-23 at.% Al-8.5 at.% Ti alloy.

Experimental Procedure

The Fe-23 at.% Al-8.5 at.% Ti alloy was prepared in a vacuum induction furnace by using pure Fe (99.9%), Al (99.9%) and Ti (99.9%). After being homogenized at 1250° C for 48 h, the ingot was sectioned into 2-mm-thick slices. These slices were subsequently solution heat-treated at 1100°C for 1 h and then quenched into room-temperature water rapidly. The aging processes were performed at 900° C for various times in a vacuum heat-treated furnace and then quenched rapidly. TEM specimens were prepared by double-jet electropolisher with an electrolyte of 67% methanol and 33% nitric acid. TEM observation was performed using a JEOL JEM-2000FX TEM operating at 200kV. Elemental concentrations were examined by using a Link ISIS 300 energy-dispersive X-ray spectrometer (EDS). Quantitative analyses of elemental concentrations for Fe, Al and Ti were made with a Cliff-Lorimer Ratio Thin Section method.

Results and Discussion

Fig. 1(a) shows a selected-area diffraction pattern of the as-quenched alloy, revealing the presence of the superlattice reflection spots of the ordered $D0_3$ phase [17]. Figs. 1(b) and (c) are (111) $D0_3$ and (200) $D0_3$ (or, equivalently, (100) B2) dark-field (DF) electron micrographs of the as-quenched alloy, exhibiting the presence of fine $D0_3$ domains with a/2<100> APBs and small B2 domains with a/4<111> APBs, respectively [15,16]. In Fig. 1(c), it is also seen that a high density of disordered A2 phase showing a dark contrast could be observed within the B2 domains. Accordingly, the as-quenched microstructure of the alloy was a mixture of ($A2+D0_3$) phases. This is similar to that reported by other workers in the as-quenched Fe-(18~22.5) at.% Al-5 at.% Ti alloys [10].

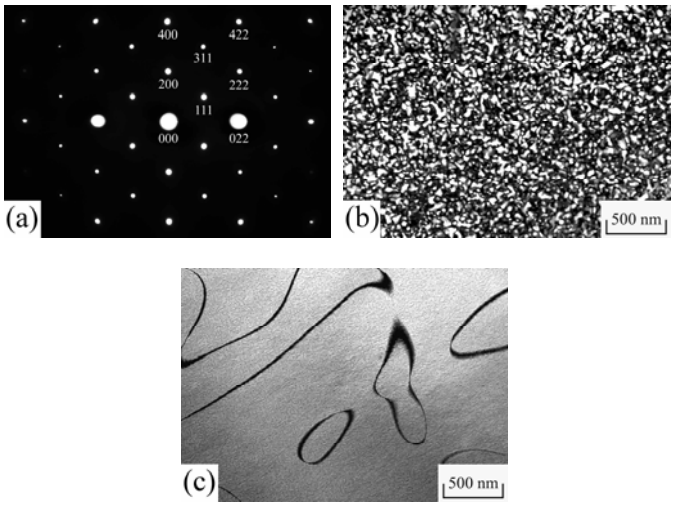

Fig. 1. Electron micrographs of the as-quenched alloy: (a) a selected-area diffraction pattern. The foil normal is [0 1 $\bar{1}$]. (hkl = $D0_3$ phase.), (b) and (c) (111) and (200) $D0_3$ DF, respectively.

When the as-quenched alloy was aged at 900° C for a short time, the $D0_3$ domains grew with preferred orientation, as shown in Fig. 2. This feature is similar to that reported by other

workers in the aged Fe-Al-Ti alloys [10]. In Fig. 2, it is also seen that the a/2<100> APBs were coated with a continuous layer of the disordered A2 phase. However, after prolonged aging at 900° C, some fine particles started to appear within the A2 phase. Figs. 3(a) and (b) are (111) and (200) $D0_3$ DF electron micrographs of the alloy aged at 900° C for 1 h, clearly revealing that the (111) $D0_3$ DF image and (200) $D0_3$ DF image are morphologically identical. Since the (200) reflection spot comes from both the B2 and $D0_3$ phases [10,12], while the (111) reflection spot comes only from $D0_3$ phase, the fine bright particles at a/2<100> APBs presented in Figs. 3(a) and (b) are considered to be $D0_3$ phase. TEM examinations indicated that no evidence of the a/4<111> APBs could be observed. This result seems to imply that the B2 domains would grow up to the whole grains during aging. With increasing the aging time at 900° C, the amount of the $D0_3$ particles at a/2<100> APBs increased and the disordered A2 phase decreased, as illustrated in Fig. 4. Fig. 5(a), (111) $D0_3$ DF electron micrograph of the alloy aged at 900° C for 24 h, indicates that at a/2<100> APBs, the amount of the $D0_3$ particles increased considerably and a dark contrast could also be detected between the particles. However, a (200) $D0_3$ DF electron micrograph (Fig. 5(b)) reveals that the whole regions of the a/2<100> APBs were full bright in contrast. This indicates that the dark regions at a/2<100> APBs presented in Fig. 5(a) should be of the B2 phase. Consequently, when the alloy was aged at 900° C for longer time, the microstructure at the a/2<100> APBs was a mixture of (B2+$D0_3$) phases.

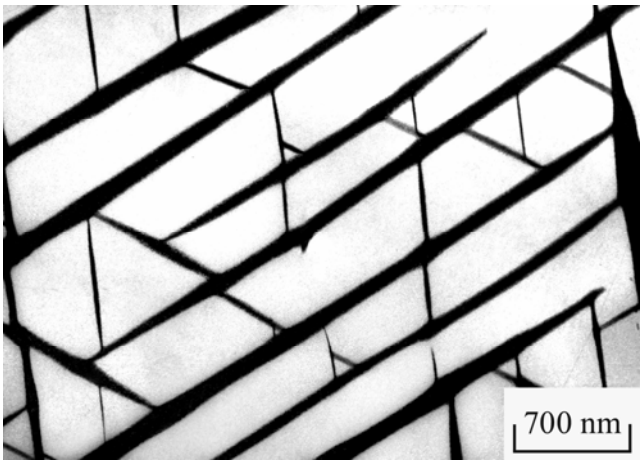

Fig. 2. (2 0 0) $D0_3$ DF electron micrograph of the alloy aged at 900°C for 0.5 h.

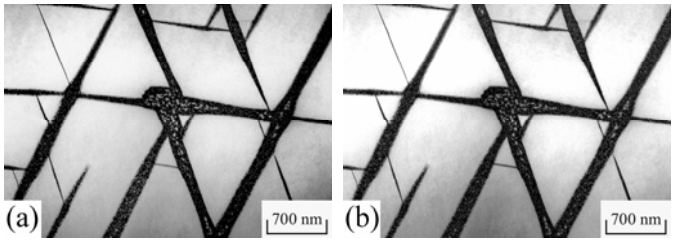

Fig. 3. Electron micrographs of the alloy aged at 900°C for 1 h. (a) and (b) (111) and (200) $D0_3$ DF, respectively.

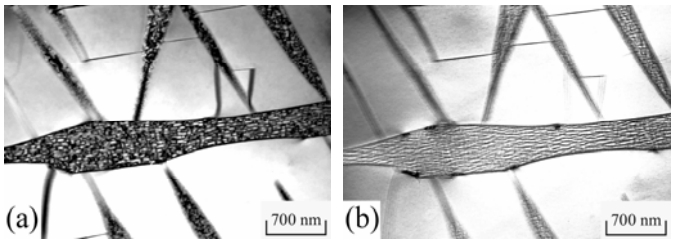

Fig. 4. Electron micrographs of the alloy aged at 900° C for 6 h. (a) and (b) (111) and (200) $D0_3$ DF, respectively.

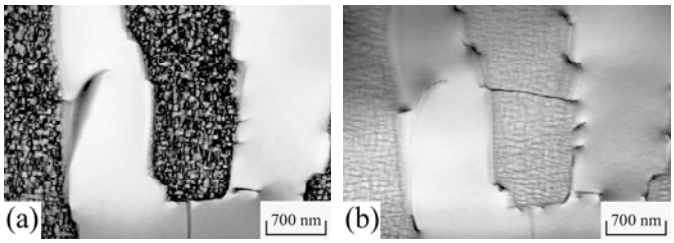

Fig. 5. Electron micrographs of the alloy aged at 900° C for 24 h. (a) and (b) (111) and (200) $D0_3$ DF, respectively.

The fact that with increasing aging time at 900° C the size of the $D0_3$ domains existing in the as-quenched alloy increased and an A2 → (A2+$D0_3$) → (B2+$D0_3$) transition occurred at a/2<100> APBs is a remarkable feature in the present study. This feature has never been reported by previous workers in the Fe-Al-Ti alloy systems before. In order to clarify this feature, the quantitatively EDS analyses were undertaken. The results are shown in Table 1. It is seen in Table 1 that when the alloy was aged at 900° C for 0.5 h, the Al and Ti concentrations in the $D0_3$ domains were much greater than those in the as-quenched alloy, and these concentrations were noticeably lower at a/2<100> APBs. The insufficient concentrations of both Al and Ti would cause the disordered A2 phase to form at a/2<100> APBs. However, along with the growth of the $D0_3$ domains, partial Al and Ti atoms would proceed to diffuse toward the a/2<100> APBs. EDS analyses indicated that during the early stage of isothermal aging at 900 ° C, the increased amount of Ti at a/2<100> APBs was more than that of Al. It implies that during aging, Ti redistributed first and then Al started to move appreciably. This result is consistent with that found by other workers in the Fe-Al-Ti ternary alloys [18], in which they reported that the diffusion of Ti is faster than that of Al. Furthermore, it is well-known that a small amount of Ti addition in the Fe-Al binary alloys would strongly enhance the formation of the $D0_3$ phase [10-12]. Therefore, it is plausible to suggest that the drastic increase of Ti concentration should be favorable for the formation of the fine $D0_3$ particles at a/2<100> APBs, which is consistent with the observation in Fig. 3. With increasing aging time at 900° C, both Al and Ti concentrations at a/2<100> APBs continue to increase significantly. It is thus expected that owing to the increase of Al and Ti, the amount of the fine $D0_3$ particles at a/2<100> APBs would increase and the microstructure of the remaining regions would transform from the disordered A2 phase to B2 phase, as observed in Figs. 4 and 5.

Finally, it is interesting to note that compared to the previously established isothermal sections of the Fe-Al-Ti

ternary alloys at 900˚C, the chemical compositions of Fe-23.8 at.% Al-11.1 at.% Ti and Fe-22.4 at.% Al-7.4 at.% Ti obtained from the $D0_3$ domain and ($B2+D0_3$) region in the present alloy aged at 900˚C for 24 h are just located in the $D0_3$ and ($B2+D0_3$) regions, respectively [12].

Table 1
Chemical Compositions of the Phases Revealed by EDS

Heat Treatment	Phase	Chemical Compositions (at.%)		
		Fe	Al	Ti
as-quenched	$A2+D0_3$	68.3	23.1	8.6
900°C, 0.5 h	$D0_3$ domain	62.5	25.1	12.4
	APB(A2)	75.9	19.8	4.3
900°C, 1 h	$D0_3$ domain	63.5	24.9	11.6
	APB($A2+D0_3$)	73.6	20.2	6.2
900°C, 6 h	$D0_3$ domain	64.4	24.3	11.3
	APB($A2+B2+D0_3$)	71.6	21.5	6.9
900°C, 24 h	$D0_3$ domain	65.1	23.8	11.1
	APB($B2+D0_3$)	70.2	22.4	7.4

Conclusions

The as-quenched microstructure of the Fe-23 at.% Al-8.5 at.% Ti alloy was a mixture of ($A2+D0_3$) phases. When the alloy was aged at 900˚ C, the $D0_3$ domains existing in the as-quenched alloy grew and an A2 → ($A2+D0_3$) → ($B2+D0_3$) transition occurred at a/2<100> APBs of the $D0_3$ domains. The microstructural revolution has never been reported by other workers in the Fe-Al-Ti alloy systems before.

Acknowledgements

The authors are pleased to acknowledge the financial support of this research by the National Science Council, Republic of China under Grant NSC 97-2221-E-009-027-MY3. They are also grateful to M.H. Lin for typing the manuscript.

References

[1] F. Dobeš, P. Kratochvíl, K. Milička, Intermetallics 14 (2006) 1199.
[2] S.M. Zhu, K. Sakamoto, M. Tamura, K. Iwasaki, Scripta Mater. 42 (2000) 905.
[3] U. Prakash, G. Sauthoff, Intermetallics 9 (2001) 107.
[4] M. Palm, G. Sauthoff, Intermetallics 12 (2004) 1345.
[5] M. Palm, J. Lacaze, Intermetallics 14 (2006) 1291.
[6] F. Stein, A. Schneider, G. Frommeyer, Intermetallics 11 (2003) 71.
[7] L. Anthony, B. Fultz, Acta Metall. Mater. 43 (1995) 3885.
[8] M. Palm, Intermetallics 13 (2005) 1286.
[9] Y. Nishino, S. Asano, T. Ogawa, Mater. Sci. Eng. A 234-236 (1997) 271.
[10] M.G. Mediratta, S.K. Ehlers, H.A. Lipsitt, Metall. Trans. A 18 (1987) 509.
[11] G. Ghosh, in: G. Effenberg (Eds.), Ternary Alloy Systems, Springer Berlin Heidelberg, New York, 2005, pp. 426-452.
[12] I. Ohnuma, C.G. Schön, R. Kainuma, G. Inden, K. Ishida, Acta Mater. 46 (1998) 2083.
[13] S.M. Zhu, K. Sakamoto, M. Tamura, K. Iwasaki, Mater. Trans. JIM. 42 (2001) 484.
[14] O. Ikeda, I. Ohnuma, R. Kainuma, K. Ishida, Intermetallics 9 (2001) 755.
[15] S.M. Allen, J.W. Cahn, Acta Metall. 24 (1976) 425.
[16] P.R. Swann, W.R. Duff, R.M. Fisher, Metall. Trans. 3 (1972) 409.
[17] C.H. Chen, T.F. Liu, Metall. Trans. A 34 (2003) 503.
[18] J. Ni, T. Ashino, S. Iwata, Acta Mater. 48 (2000) 3193.

Formation of (B2+$D0_3$) two-phase microstructure in a Fe-23 Al-7 Ti alloy

Chun-Wei Su, Chih-Lung Lin, Kai-Ming Chang, Po-Chih Chen, Yung-Chang Chen, Cheng-Yi Lin, C.G. Chao and T.F. Liu*
Department of Materials Science and Engineering, National Chiao Tung University,
(NSC 97-2221-E-009-027-MY3)

Abstract

As-quenched microstructure of the Fe-23at.% Al-7at.% Ti alloy was a mixture of (A2+$D0_3$) phases. When the as-quenched alloy was aged at 1073K for moderate times, $D0_3$ domains grew preferentially along <100> directions and extremely fine B2 particles occurred at a/2<100> anti-phase boundaries (APBs). After prolonged aging at 1073K, the B2 particles would grow to occupy the whole a/2<100> APBs. Consequently, the stable microstructure of the alloy at 1073K was a mixture of (B2+$D0_3$) phases.

Keywords: *phase transformation, electron microscopy, microstructure*

Introduction

Effects of Ti addition on the microstructures of the Fe-rich Fe-Al binary alloys have been extensively studied by many workers.[1-9)] Based on these studies, it can be generally concluded that the addition of Ti in the Fe-Al binary alloys would not only pronouncedly raise the A2+$D0_3$ (or $D0_3$)→B2→A2 transition temperatures but also significantly expand the (A2+$D0_3$) phase field.[3-9)] In addition, a (B2+$D0_3$) two-phase field was reported to be detected in the Fe-Al-Ti ternary alloys.[7-9)] Interestingly, the (B2+$D0_3$) two-phase field has not been found by previous workers in the Fe-Al binary alloys before.[10-12)] However, to date, the existence of the (B2+$D0_3$) two-phase field in the Fe-Al-Ti ternary alloys was determined principally by means of X-ray diffraction and electron-probe microanalysis (EPMA).[7-9)] Little transmission electron microscopy (TEM) information concerning the formation of the (B2+$D0_3$) two-phase microstructure has been provided in the literature. Therefore, the purpose of this work is an attempt to clarify the microstructural development for the formation of (B2+$D0_3$) phases in the Fe-23at.% Al-7at.% Ti alloy by TEM observation.

Experimental Procedure

(The Fe-23at.% Al-7at.% Ti alloy was prepared in a vacuum induction furnace by using high purity (99.99%) constituent elements. After being homogenized at 1523K for 48h, the ingot was sectioned into 2-mm-thick slices. These slices were subsequently solution heat-treated at 1373K for 1h and then rapidly quenched into room-temperature water. The aging processes were performed at 1073K for various times in a vacuum heat-treated furnace and then quenched rapidly. TEM specimens were prepared by means of double-jet electropolisher with an electrolyte of 67% methanol and 33% nitric acid. TEM observation of microstructure was performed on a JEOL JEM-2000FX TEM operating at 200kV. This microscope was equipped with a Link ISIS 300 energy-dispersive X-ray spectrometer (EDS) for chemical analysis. Quantitative analyses of elemental concentrations were made with a Cliff-Lorimer Ratio Thin Section method.

Results and Discussion

An optical micrograph of the as-quenched alloy is shown in Figure 1(a). Figure 1(b) is a selected-area diffraction pattern (SADP) of the as-quenched alloy, exhibiting the superlattice reflection spots of the ordered $D0_3$ phase.[13,14)] Figure 1(c) is a $(1\bar{1}1)$ $D0_3$ dark-field (DF) electron micrograph, revealing the presence of fine $D0_3$ domains with a/2<100> APBs. Figure 1(d), a (200) $D0_3$ DF electron micrograph, shows the presence of small B2 domains with a/4<111> APBs. Since the sizes of both $D0_3$ and B2 domains are small, it is suggested that these domains were formed during quenching.[11-17)] In Figure 1(d), it is also seen that a high density of disordered A2 phase (dark contrast) was present within the B2 domains; otherwise there would be no dark contrast within these domains by using a (200) superlattice reflection. Therefore, it is concluded that the as-quenched microstructure of the alloy was a mixture of (A2+$D0_3$) phases which were formed by an A2→B2→(A2+$D0_3$) transition during quenching. This result is similar to that reported by Mendiratta *et al.* in the Fe-(18~25)at.% Al-5at.% Ti alloys quenched from 1373K.[3)]

When the as-quenched alloy was aged at 1073K, the $D0_3$ domains grew rapidly, as illustrated in Figure 2. Figure 2(a) is a DF electron micrograph obtained by use of the (200) superlattice reflection in [001] zone, revealing that the $D0_3$ domains grew preferentially along <100> crystallographic directions. This feature is also similar to that observed by Mendiratta *et al.*.[3)] Figure 2(b), $(1\bar{1}1)$ $D0_3$ DF electron micrograph of the same area as Figure 2(a) with a higher magnification, shows that the a/2<100> APBs are fully dark in contrast. Figure 2(b), a (200) $D0_3$ DF electron micrograph, reveals that a high density of extremely fine particles could be observed at the a/2<100> APBs. Since the amount of the

particles was very small, the reflection spots of the particles were very faint. In order to carry out an unambiguous identification about the particles, prolonged aging at 1073K was performed.

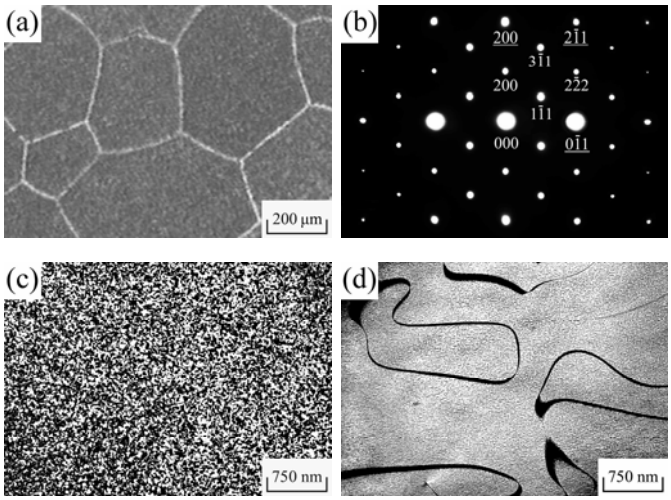

Figure 1 (a) An optical micrograph of the as-quenched alloy, (b) through (d) electron micrographs of the as-quenched alloy: (b) an SADP. The foil normal is [011]. (*hkl*: disordered A2, ***hkl*:** $D0_3$ phase.), (c) and (d) $(1\,\bar{1}\,1)$ and $(2\,0\,0)$ $D0_3$ DF, respectively.

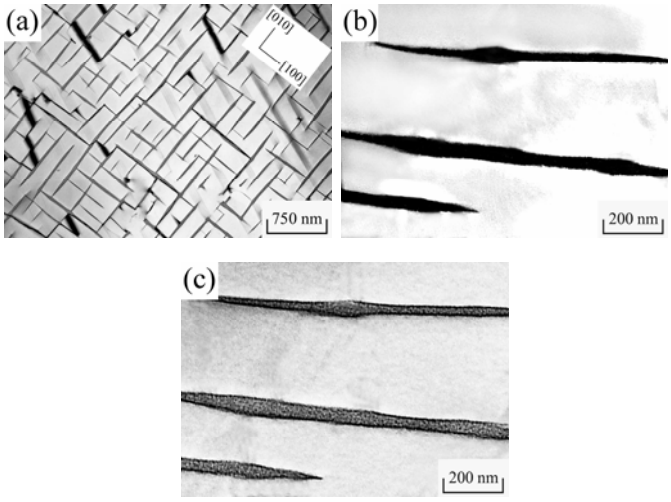

Figure 2 Electron micrographs of the alloy aged at 1073K for 1 h: (a) $(2\,0\,0)$ $D0_3$ DF, (b) and (c) $(1\,\bar{1}\,1)$ and $(2\,0\,0)$ $D0_3$ DF with a higher magnification of (a), respectively.

Figure 3(a) is a bright-field (BF) electron micrograph of the alloy aged at 1073K for 16h. In this figure, it is clear that the domains had grown to be very large and the morphology changed from cubic to granular shape. Figures 3(b) and 3(c) are two SADPs taken from the areas marked as "D" and "B" in Figure 3(a), respectively. In our previous study,[17] it was found that the intensity of the $(1\,\bar{1}\,1)$ and (200) reflection spots of a single $D0_3$ phase should be almost equivalent. Therefore, it seems to be deduced that the reflection spots present in Figure 3(b) should be of a single $D0_3$ phase. However, it is clearly seen in Figure 3(c) that the (200) and $(2\bar{2}2)$ reflection spots are much stronger than the $(1\,\bar{1}\,1)$ reflection spot. Therefore, it is strongly suggested that the (200) and $(2\bar{2}2)$ reflection spots should derive from not only $D0_3$ phase but also the B2 phase, since the $(1\,\bar{1}\,1)$ reflection spot comes from the $D0_3$ phase only; while the (200) and $(2\bar{2}2)$ reflection spots can come from both the $D0_3$ and B2 phases (the (200) and $(2\bar{2}2)$ $D0_3$ reflection spots are equal to the (100) and $(1\,\bar{1}\,1)$ B2 reflection spots, respectively).[11,12] Figures 3(d) and (e) are $(1\,\bar{1}\,1)$ and (200) $D0_3$ DF electron micrographs of the same area as in Figure 3(a). It is obviously seen that at the regions marked as "D", the $(1\,\bar{1}\,1)$ DF image and the (200) DF image are morphologically identical, and these domains are fully bright in contrast. It means that these domains are of single $D0_3$ phase; whereas, at the regions marked as "B", the B2 particles are much larger than those observed at a/2<100> APBs in Figure 2(b), and the $D0_3$ particles are very extremely fine. This indicates that at the regions marked as "B", the B2 particles were existent at the aging temperature, and the extremely fine $D0_3$ particles were formed during quenching from the quenching temperature by a B2→$D0_3$ ordering transition.[11-17] With increasing the aging time at 1073K, besides the presence of the well-grown $D0_3$ domains, the B2 particles would grow to occupy the whole a/2<100> APBs and extremely fine quenched-in $D0_3$ particles could be also detected within the B2 particles. A typical microstructure is illustrated in Figure 4. Accordingly, the stable microstructure of the alloy present at 1073K was a mixture of (B2+$D0_3$) phases.

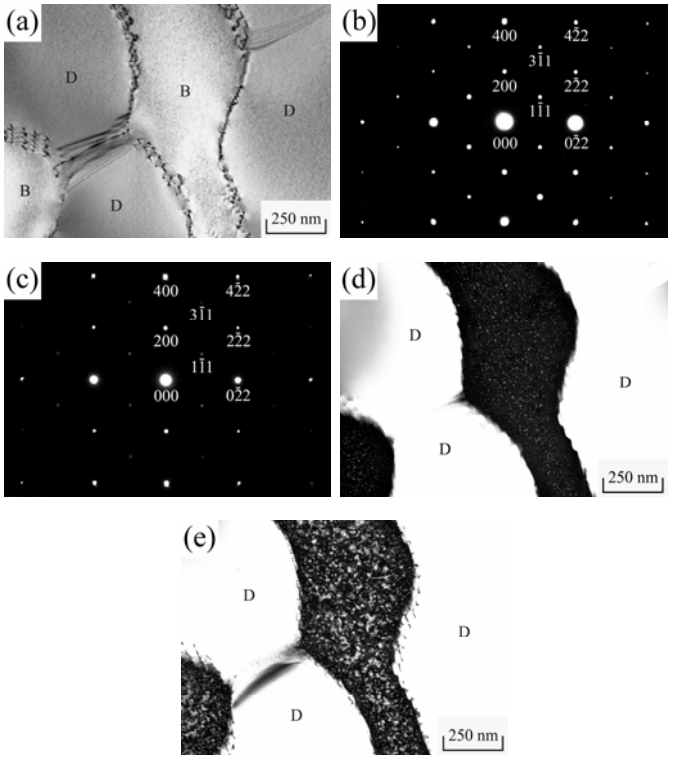

Figure 3 Electron micrographs of the alloy aged at 1073K for 16 h: (a) BF, (b) and (c) two SADPs taken from the areas marked as "D" and "B" in (a), respectively. (*hkl*: $D0_3$ phase), (d) and (e) $(1\,\bar{1}\,1)$ and (200) $D0_3$ DF, respectively.

Based on the preceding results, it is clear that when the present alloy was aged at 1073K for longer times, the $D0_3$ domains existing in the as-quenched alloy grew and the B2 phase started to occur at the a/2<100> APBs. This transition behavior has never been observed by other workers in the Fe-Al and Fe-Al-Ti alloy systems before. In order to clarify this feature, EDS analyses were undertaken. The average concentrations of the alloying elements were obtained from at least ten different EDS profiles of each phase. The results are summarized in Table 1.

Table 1
Chemical compositions of the phases revealed by Energy-Dispersive X-ray Spectrometer (EDS)

Heat Treatment	Phase(s)	Chemical compositions (at.%)		
		Fe	Al	Ti
as-quenched	A2+$D0_3$	69.90	23.08	7.02
1073K, 72 h	$D0_3$	65.76	24.15	10.09
1073K, 72 h	B2	76.35	20.13	3.52

Obviously, it is seen in Table 1 that both the Al and Ti concentrations in the $D0_3$ phase are much greater than those in the as-quenched alloy. It is thus expected that along with the growth of the $D0_3$ domains, the concentrations of both Al and Ti at a/2<100> APBs would be lacked. The EDS examinations indicated that the elemental concentrations of Al and Ti in the B2 phase are 20.13 and 3.52at.%, respectively. According to the phase diagram of Fe-Al binary alloys,[11,12] it is seen that the microstructure of an Fe-20.13at.% Al alloy existing at 1073K should be a single disordered A2 phase, and no evidence of B2 phase could be observed. Therefore, it is plausible to suggest that the existence of 3.52at.% Ti at a/2<100> APBs would be favorable for the formation of the B2 phase, rather than the A2 phase.

Finally, it is worthwhile to point out that the B2→$D0_3$ ordering transition could be found to occur in the Fe-Al binary alloys with Al > 25at.%.[12] However, it is clear in Figure 4 that the B2→$D0_3$ ordering transition could be detected and the Al content in the B2 phase was examined to be 20.13at.% only. This result implies that the existence of Ti would significantly lead the B2→$D0_3$ ordering transition to occur with lower Al content.

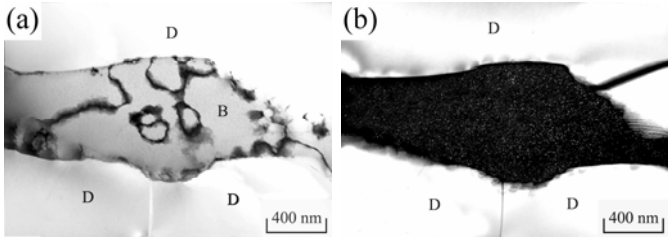

Figure 4 (a) and (b) ($2\,0\,0$) and ($1\,\bar{1}\,1$) $D0_3$ DF electron micrographs of the alloy aged at 1073K for 72 h.

Conclusions

The as-quenched microstructure of the Fe-23at.% Al-7at.% Ti alloy was a mixture of (A2+$D0_3$) phases. The (A2+$D0_3$) phases were formed by an A2→B2→(A2+$D0_3$) transition during quenching. When the alloy was aged at 1073K for moderate times, the $D0_3$ domains grew preferentially along <100> directions and extremely fine B2 particles occurred at a/2<100> APBs. After prolonged aging at 1073K, the B2 particles would grow to occupy the whole a/2<100> APBs. Consequently, the stable microstructure of the alloy present at 1073K was a mixture of (B2+$D0_3$) phases.

Acknowledgements

The authors are pleased to acknowledge the financial support of this research by the National Science Council, Republic of China under Grant NSC 97-2221-E-009-027-MY3. They are also grateful to M.H. Lin for typing the manuscript.

References

[1] U. Prakash and G. Sauthoff: Intermetallics **9** (2001) 107-112.
[2] M. Palm and J. Lacaze: Intermetallics **14** (2006) 1291-1303.
[3] M.G. Mediratta, S.K. Ehlers and H.A. Lipsitt: Metall. Trans. A **18** (1987) 509-518.
[4] Y. Nishino, S. Asano and T. Ogawa: Mater. Sci. Eng. A **234-236** (1997) 271-274.
[5] M. Palm: Intermetallics **13** (2005) 1286-1295.
[6] F. Stein, A. Schneider and G. Frommeyer: Intermetallics **11** (2003) 71-82.
[7] S.M. Zhu, K. Sakamoto, M. Tamura and K. Iwasaki: Mater. Trans. JIM. **42** (2001) 484-490.
[8] I. Ohnuma, C.G. Schön, R. Kainuma, G. Inden and K. Ishida: Acta Mater. **46** (1998) 2083-2094.
[9] G. Ghosh: *Ternary Alloy Systems*, (Springer Berlin Heidelberg New York, 2005) pp. 426-452.
[10] O. Ikeda, I. Ohnuma, R. Kainuma and K. Ishida: Intermetallics **9** (2001) 755-761.
[11] S.M. Allen and J.W. Cahn: Acta Mater. **24** (1976) 425-437.
[12] P.R. Swann, W.R. Duff and R.M. Fisher: Metall. Trans. **3** (1972) 409-419.
[13] C.H. Chen and T.F. Liu: Metall. Trans. A **34** (2003) 503-509.
[14] C.H. Chen and T.F. Liu: Scripta Mater. **47** (2002) 515-520.
[15] S.Y. Yang and T.F. Liu: Scripta Mater. **54** (2006) 931-935.
[16] T.F. Liu, J.S. Chou and C.C. Wu: Metall. Trans. A **21** (1990) 1891-1899.
[17] S.Y. Yang and T.F. Liu: J. Alloys Compd. **417** (2006) 63-68.

Phase separation from $L2_1$ to (B2+$L2_1$) in Fe-24.6Al-7.5Ti alloy

Gow-Dong Tsay*, Chih-Lung Lin, Kai-Ming Chang, Po-Chih Chen, Yung-Chang Chen, Cheng-Yi Lin, Chuen-Guang Chao and Tzeng-Feng Liu*

Department of Materials Science and Engineering, National Chiao Tung University

(NSC 97-2221-E-009-027-MY3)

Abstract

As-quenched microstructure of the Fe-24.6 at.% Al-7.5 at.% Ti alloy was a mixture of (A2+$L2_1$) phases. When the as-quenched alloy was aged at 1173K for moderate times, the $L2_1$ domains grew considerably and B2 phase was formed at a/2<100> anti-phase boundaries (APBs) as well as phase separation from well-grown $L2_1$ to (B2+$L2_1^*$) occurred basically contiguous to the APBs, where $L2_1^*$ is also a $L2_1$-type phase. With continued aging at 1173K, the phase separation would proceed toward the whole well-grown $L2_1$ domains. This microstructural evolution has not been reported in the Fe-Al-Ti alloy systems before.

Keywords: iron aluminum titanium alloys, phase transformations, transmission electron microscopy, phase separation

Introduction

In previous studies,[1-11] it is seen that the Ti addition in the Fe-Al binary alloys would (1) strongly increase the $D0_3$→B2 and B2→A2 transition temperatures,[1-10] (2) significantly expand the (A2+$D0_3$) phase field,[5-7] and (3) cause the $D0_3$ APBs to exhibit a tendency toward anisotropy.[6] In addition, a (B2+$L2_1$) ($L2_1$ is the ternary equivalent of the binary $D0_3$ structure.[3]) two-phase field was reported to be existent at temperatures ranging from 1073 to 1273K in the Fe-Al-Ti ternary alloys.[7-11] It is noted that the (B2+$D0_3$) two-phase field has not been found by previous workers in the Fe-Al binary alloys before.[12-13] However, the existence of the (B2+$L2_1$) two-phase field in the Fe-Al-Ti ternary alloys was determined principally by using X-ray diffraction, differential scanning calorimetry, differential thermal analysis and electron-probe microanalysis.[7-11] Recently, we have performed transmission electron microscopy (TEM) investigations on the phase transformations of a Fe-23 at.% Al-8.5 at.% Ti alloy aged at 1173K.[14] Consequently, it was found that when the alloy was aged at 1173K for longer times, the $L2_1$ domains grew considerably and an A2→(A2+$L2_1$)→(B2+$L2_1$) transition occurred at a/2<100>APBs. This feature has never been reported by other workers in the Fe-Al-Ti alloy systems before. Extending the previous work, the purpose of this study is an attempt to examine the microstructural developments of the Fe-24.6 at.% Al-7.5 at.% Ti alloy aged at 1173K. It is noted that according to the previously established isothermal sections of Fe-Al-Ti ternary alloys at 1173K,[6-11] the chemical compositions of both the previous alloy and the present alloy are just located in the (B2+$L2_1$) region. However, the chemical composition of the present alloy is much closer to the A2/B2/$L2_1$ apex than that of the previous alloy.

Experimental Procedure

The Fe-24.6 at.% Al-7.5 at.% Ti alloy was prepared in a vacuum induction furnace by using Fe(99.9%), Al(99.9%) and Ti(99.9%). After being homogenized at 1523K for 48 h, the ingot was sectioned into 2-mm-thick slices. These slices were subsequently solution heat-treated at 1373K for 1 h and then quenched into room-temperature water rapidly. The aging processes were performed at 1173K for various times in a vacuum heat-treated furnace and then quenched rapidly. TEM specimens were prepared by means of double-jet electropolisher with an electrolyte of 67% methanol and 33% nitric acid. Electron microscopy was performed on a JEOL JEM-2000FX scanning transmission electron microscope (STEM) operating at 200kV. This microscope was equipped with a Link ISIS 300 energy-dispersive X-ray spectrometer (EDS) for chemical analysis. Quantitative analyses of elemental concentrations for Fe, Al and Ti were made with the aid of a Cliff-Lorimer ratio thin section method.

Results and Discussion

Figure 1(a) is a selected-area diffraction pattern of the as-quenched alloy, exhibiting the superlattice reflection spots of the ordered $L2_1$ phase.[14-16] Figures 1(b) and (c) are (200) $L2_1$ (or, equivalently, (100) B2) and (111) $L2_1$ dark-field (DF) electron micrographs of the as-quenched alloy, showing the presence of the small B2 domains and fine $D0_3$ domains, respectively.[12,13] In Figures 1(b) and (c), it is seen that the sizes of both B2 and $L2_1$ domains are very small, indicating that these domains were formed during quenching.[12,13] In Figure 1(b), it is also seen that a high density of extremely fine disordered A2 phase (dark contrast) could be observed within the B2 domains; otherwise, there would be no contrast within these domains by using a (200) superlattice reflection.[6] Accordingly, the as-quenched microstructure of the alloy was a mixture of (A2+$L2_1$) phases. This is similar to that observed by the present workers in the Fe-23 at.% Al-8.5 at.% Ti alloy quenched from 1373K.[14]

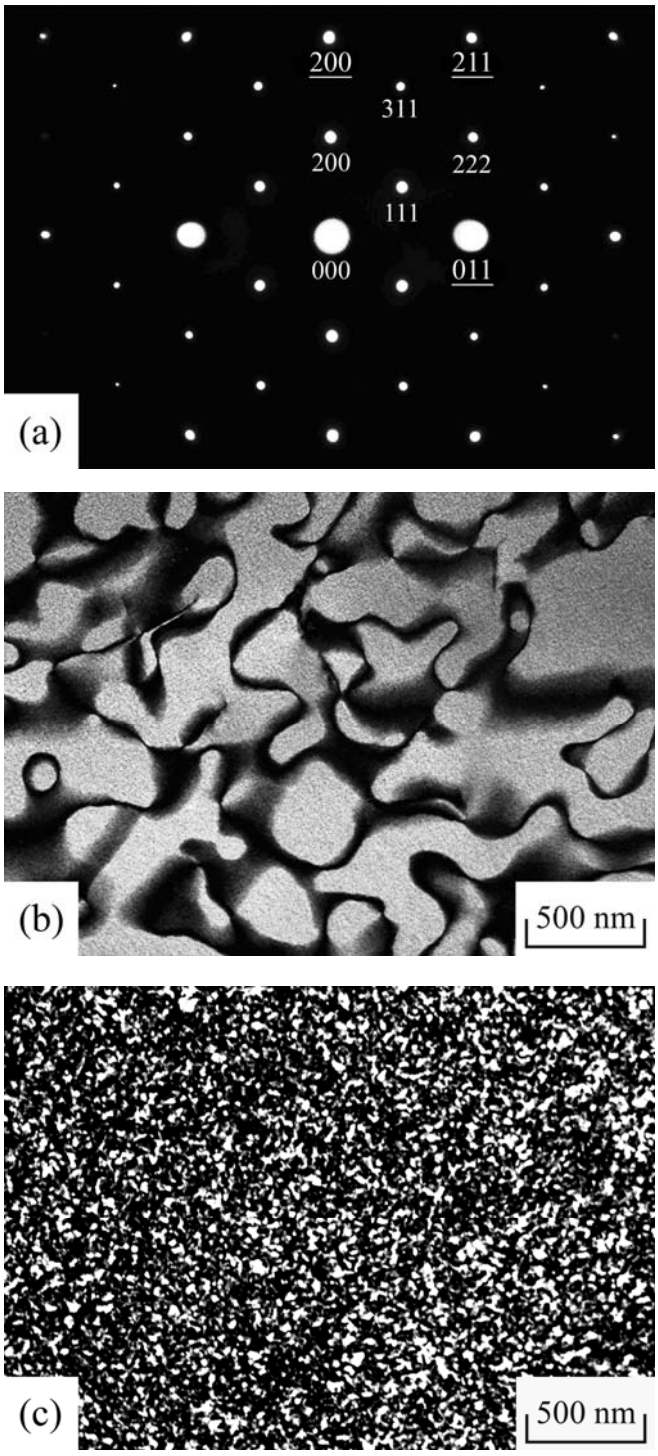

Fig.1 Electron micrographs of the as-quenched alloy: (a) a selected-area diffraction pattern. The foil normal is [01 $\bar{1}$]. (*hkl*: disordered A2, *hkl*: $L2_1$ phase); (b) and (c) (200) and (111) $L2_1$ DF, respectively.

Figure 2 is a (111) $L2_1$ DF electron micrograph of the alloy aged at 1173K for 3 h, clearly revealing that the $L2_1$ domains grew significantly and a/2<100> APBs were coated with the disordered A2 phase. However, after prolonged aging at 1173K, some tiny particles started to form within the A2 phase. A typical example is shown in Figure 3. Figures 3(a) and (b) are (111) and (200) $L2_1$ DF electron micrographs of the alloy aged at 1173K for 6 h, showing that the (111) DF image and the (200) DF image are morphologically identical. Therefore, it is likely to conclude that the microstructure of the alloy aged at 1173K for 6 h was also $L2_1$ phase and the a/2<100> APBs were coated with the disordered A2 phase. However, the (111) $L2_1$ DF electron micrograph of the same area as Figure 3(a) with a higher magnification revealed that the a/2<100> APBs were fully dark in contrast, as shown in Figure 3(c); whereas the (200) $L2_1$ DF electron micrograph showed that some tiny particles (indicated with arrows) could be observed at the a/2<100> APBs, as illustrated in Figure 3(d). Therefore, it is reasonable to deduce that the tiny bright particles present in Figure 3(d) should be of B2 phase, since the (111) reflection spot comes from the $L2_1$ phase only; while the (200) reflection spot can come from both the $L2_1$ and B2 phases.[12,13] With continued aging at 1173K, the $L2_1$ domains continued to grow and a phase separation started to occur basically contiguous to a/2<100> APBs of the $L2_1$ domains. An example is shown in Figure 4. Figure 4(a) is a (111) $L2_1$ DF electron micrograph of the alloy aged at 1173K for 12 h, showing that the a/2<100> APBs broadened and well-grown $L2_1$ domains decomposed into fine $L2_1$ domains (designated as $L2_1^*$ phase to be distinguished from the original $L2_1$ phase) separated by dark layers. Figure 4(b) is a (200) $L2_1$ DF electron micrograph taken from the same area as Figure 4(a), clearly revealing that in addition to the presence of a few A2 particles, the whole region is bright in contrast. This indicates that the broadened dark lines on a/2<100> APBs and dark layers around the periphery of the $L2_1^*$ domains should be of the B2 phase. It is apparent that the B2 phase was formed at a/2<100> APBs and phase separation from $L2_1$ to ($B2+L2_1^*$) occurred basically contiguous to the a/2<100> APBs. Figure 5(a) is a (111) $L2_1$ DF electron micrograph of the alloy aged at 1173K for 24 h, indicating that with increasing aging time, the phase separation would proceed toward the inside of the $L2_1$ domains. Figure 5(b), (200) $L2_1$ DF electron micrograph taken from the same area as Figure 5(a), clearly reveals that only one a/2<100> APB and one A2 particle (indicated with arrows in Figures 5(a) and (b)) could be observed. Figures 6(a) and (b) are (111) and (200) $L2_1$ DF electron micrographs of the alloy aged at 1173K for 36 h, revealing that besides a little A2 phase, the well-grown $L2_1$ domains decomposed into the ($B2+L2_1^*$) phases completely.

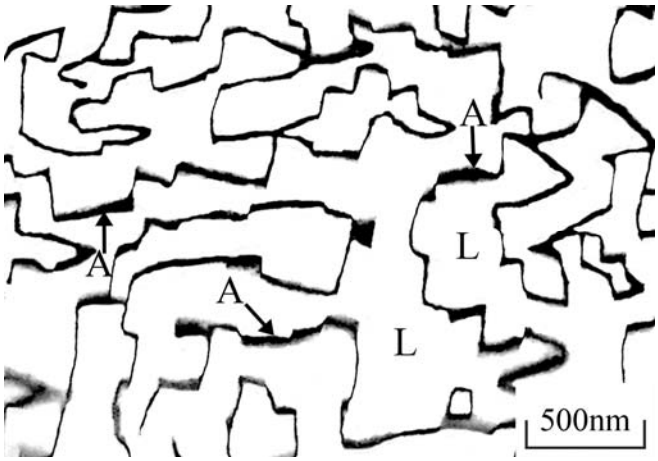

Fig.2 (111) $L2_1$ DF electron micrograph of the alloy aged at 1173K for 3 h.

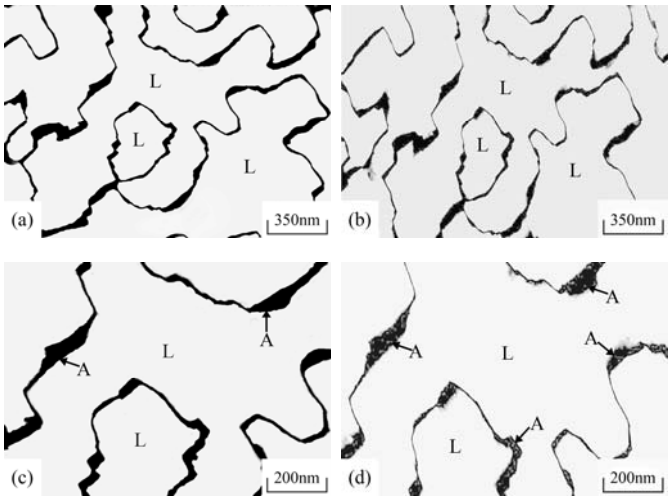

Fig.3 Electron micrographs of the alloy aged at 1173K for 6 h. (a) and (b) (111) and (200) $L2_1$ DF, respectively. (c) and (d) (111) and (200) $L2_1$ DF with a higher magnification of (a) and (b), respectively.

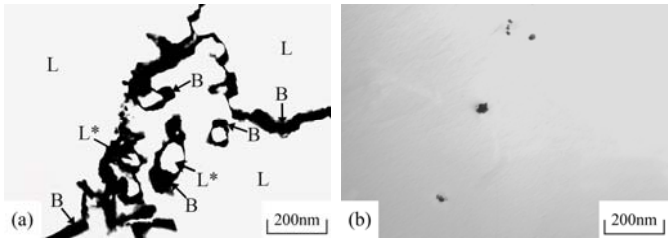

Fig.4 Electron micrographs of the alloy aged at 1173K for 12 h. (a) and (b) (111) and (200) $L2_1$ DF, respectively.

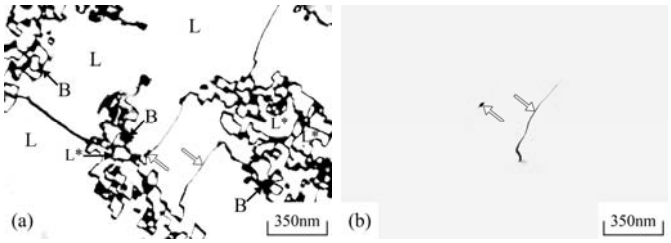

Fig.5 Electron micrographs of the alloy aged at 1173K for 24 h. (a) and (b) (111) and (200) $L2_1$ DF, respectively.

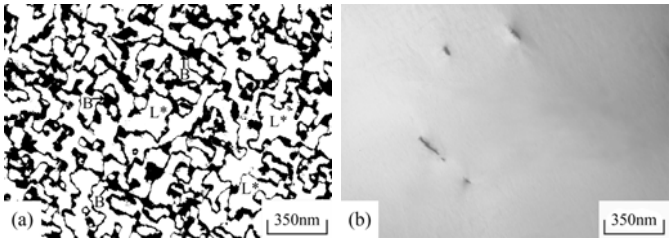

Fig.6 Electron micrographs of the alloy aged at 1173K for 36 h. (a) and (b) (111) and (200) $L2_1$ DF, respectively.

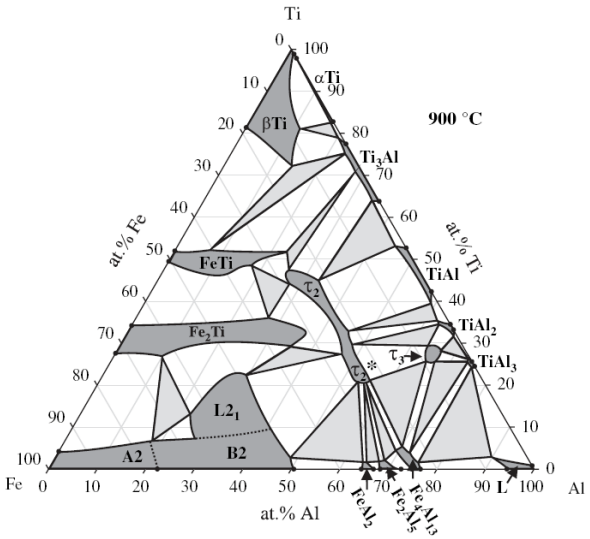

Fig.7 Isothermal section of the Fe-Al-Ti system at 1173K.[10] respectively.

Based on the above observations, some important experimental results are discussed below. When the present alloy was aged at 1173K for moderate times, the B2 phase was formed at a/2<100> APBs and phase separation from well-grown $L2_1$ to ($B2+L2_1^*$) occurred basically contiguous to the APBs. With increased aging time at 1173K, the phase separation would proceed toward the inside of the whole well-grown $L2_1$ domains. This finding is different from that observed by the present workers in the Fe-23 at.% Al-8.5 at.% Ti alloy,[14] in which we have demonstrated that when the Fe-23 at.% Al-8.5 at.% Ti alloy was aged at 1173K, the mixture of the ($B2+L2_1$) phases occurred at a/2<100> APBs and no evidence of the phase separation could be observed. In order to clarify the apparent difference, an STEM-EDS study was undertaken. The EDS analyses were taken from the areas of the $L2_1$ domains, APBs, B2 phase and $L2_1^*$ domains marked as "L", "A", "B" and "L^*" in Figures 2 through 6, respectively. The average concentrations of the alloying elements obtained by analyzing at least ten different EDS spectra of each phase are listed in Table 1. For comparison, the chemical composition of the as-quenched alloy is also listed in Table 1. It is clearly seen in Table 1 that when the alloy was aged at 1173K for 3h, the Al and Ti concentrations in the $L2_1$ domains were distinctly higher than those in the as-quenched alloy. This means that along with the growth of the $L2_1$ domains, the concentrations of both Al and Ti at a/2<100> APBs would be lacking. The insufficient concentrations of both Al (19.8 at.%) and Ti (3.8 at.%) would cause the disordered A2 phase to form at a/2<100> APBs, which is consistent with the previously established Fe-Al-Ti phase diagram as shown in Figure 7.[10] According to the phase diagram, the chemical composition of Fe-19.8 at.% Al-3.8 at.% Ti is just located in the A2 phase region. EDS analyses indicated that when the alloy was aged at 1173K for 3-12 h, the Ti concentration in the $L2_1$ domains maintained to be about 7.8 at.% and the Al concentration gradually decreased with increasing the aging time. It is thus expected that the Al atom would proceed to diffuse toward the a/2<100> APBs during aging. In Table 1, it is seen that when the alloy was aged at 1173K for 6 h, the Al concentration at a/2<100> APBs increased to 22.1 at.%. The significant increase of the Al

concentration would lead the tiny B2 particles to form at a/2<100> APBs, which is also consistent with the Fe-Al-Ti phase diagram in Figure 7.[10] In the phase diagram, it is clearly seen that the chemical composition of Fe-22.1 at.% Al-3.9 at.% Ti is close to the A2/B2 transition boundary. With increasing the aging time, the $L2_1$ domains continued to grow. The quantitative analyses revealed that the Al concentration of the $L2_1$ domains in the alloy aged for 6 h was 25.7 at.% while that for 12 h was 25.2 at.%, which gave a decrease of only 0.5 at.%. However, along with the enlargement of the $L2_1$ domain size, the volume fraction of the a/2<100> APBs would be lessened considerably. This means that the slight decrease of the Al concentration in the $L2_1$ domains would cause the Al concentration at a/2<100> APBs to increase appreciably. Therefore, it is reasonable to believe that due to the appreciable increase of the Al concentration, the A2 phase existing at a/2<100> APBs would be transformed to B2 phase,[10] as observed in Figure 4(a). TEM observations indicated that along with the formation of the B2 phase, the phase separation from well-grown $L2_1$ to (B2+$L2_1^*$) occurred basically contiguous to a/2<100> APBs. In the following description, we will attempt to discuss why the well-grown $L2_1$ domains underwent the phase separation. In the previous studies, it is well-known that the $D0_3$ phase could be found to exist in the Fe-Al binary alloys only at temperatures below 823K,[12,13] and the Ti addition in the Fe-Al binary alloys would result in a particularly large increase of the $D0_3(L2_1)\rightarrow$B2 transition temperature about 60K/at.%.[6-11] Obviously, the Ti concentration would be the predominant factor for the stabilization of the $L2_1$ phase at high temperature. In our previous study of the Fe-23 at.% Al-8.5 at.% Ti alloy aged at 1173K for 6-24 h,[14] it was found that the Ti concentration in the well-grown $L2_1$ domains was up to about 11.1 at.%, therefore, the $L2_1$ phase exhibited more stable and no evidence of the phase separation could be detected. However, when the present alloy was aged at 1173K for 6-24 h, the Ti concentration in the well-grown $L2_1$ domains was found to be only about 7.8 at.%, which is noticeably lower than that detected in the previous alloy. Therefore, it is plausible to suggest that owing to the lower Ti concentration, the well-grown $L2_1$ domains seemed not very stable at 1173K. Consequently, the well-grown $L2_1$ domains would separate to the mixture of the Ti-riched $L2_1^*$ and Ti-lacked B2 phase, as observed in Figures 4 through 6.

Table1. Chemical compositions of the phases revealed by EDS.

Heat treatment	Phase	Chemical composition (at.%)		
		Fe	Al	Ti
As-quenched	A2+$L2_1$	67.9	24.6	7.5
1173K, 3 h	$L2_1$	65.9	26.2	7.9
	APB(A2)	76.4	19.8	3.8
1173K, 6 h	$L2_1$	66.5	25.7	7.8
	APB(A2+B2)	74.0	22.1	3.9
1173K, 12 h	$L2_1$	67.0	25.2	7.8
	$L2_1^*$	66.2	25.1	8.7
	B2	69.6	24.1	6.3
1173K, 24 h	$L2_1$	67.2	25.1	7.7
	$L2_1^*$	66.2	25.0	8.8
	B2	69.6	24.2	6.2
1173K, 36 h	$L2_1^*$	66.1	25.1	8.8
	B2	69.5	24.2	6.3

Finally, three more features are worthwhile to note as follows: (1) In the previous study,[14] it is clearly seen that the a/2<100> APBs of the well-grown $L2_1$ domains exhibited more pronounced anisotropy than those observed in the present alloy. The reason is possibly that the well-grown $L2_1$ domains in the previous alloy had significantly higher Ti concentration. (2) The chemical composition of the previous alloy had higher Ti and lower Al contents.[14] When the previous alloy was aged at 1173K, the $L2_1$ domains grew rapidly and the Ti atom was the major element for diffusing into the a/2<100> APBs. This effect caused the tiny $L2_1$ particles to precipitate preferentially at a/2<100> APBs.[14] However, when the present alloy was aged at 1173K, the Ti concentration in the well-grown $L2_1$ domains maintained to be about 7.8 at.% and the Al atom played the dominant role to diffuse into the a/2<100> APBs. Therefore, the tiny B2 particles were found to form at the a/2<100> APBs, rather than $L2_1$ particles. (3) According to the Fe-Al-Ti phase diagrams,[6-11] the A2 phase can not appear for the Fe-24.6 at.% Al-7.5 at.% Ti alloy. However, a little A2 phase was always observed in the present alloy aged at 1173K for 12-36 h. The reason for the difference is plausibly that the phase diagrams were determined by the Fe-Al-Ti alloys heat-treated at 1173K for a time period longer than 336 h, whereas the present alloy was aged for 36 h only. Actually, in the present study, it was found that when the as-quenched alloy was aged at 1173K for 3-36 h, the amount of the A2 phase was indeed decreased with increasing the aging time.

Conclusions

In the as-quenched condition, the microstructure of the Fe-24.6 at.% Al-7.5 at.% Ti alloy was the mixture of (A2+$L2_1$) phases. When the as-quenched alloy was aged at 1173K for 6 h, the $L2_1$ domains grew considerably and the B2 phase was formed at a/2<100> APBs as well as the phase separation from well-grown $L2_1$ to (B2+$L2_1^*$) occurred basically contiguous to the a/2<100> APBs. After prolonged aging at 1173K, the phase separation would proceed toward the inside of the whole well-grown $L2_1$ domains. Consequently, the microstructure of the alloy aged at 1173K for 36 h was essentially the mixture of (B2+$L2_1^*$) phases.

Acknowledgements

The authors are pleased to acknowledge the financial support of this research by the National Science Council, Republic of China under Grant NSC 97-2221-E-009-027-MY3.

References

1) Y. Nishino, S. Asano, T. Ogawa, Mater. Sci. Eng. **A 234–236** (1997) 271-274.
2) F. Stein, A. Schneider, G. Frommeyer, Intermetallics **11** (2003) 71-82.
3) M. Palm, Intermetallics **13** (2005) 1286-1295.
4) L. Anthony, B. Fultz, Acta Metall. Mater. **43** (1995) 3885-3891.
5) O. Ikeda, I. Ohnuma, R. Kainuma, K. Ishida, Intermetallics **9** (2001) 755-761.
6) M.G. Mendiratta, S.K. Ehlers, H.A. Lipsitt, Metall. Trans. A **18** (1987) 509-518.
7) I. Ohnuma, C.G. Schon, R. Kainuma, G. Inden, K. Ishida, Acta Mater. **46** (1998) 2083-2094.

8) S.M. Zhu, K. Sakamoto, M. Tamura, K. Iwasaki, Mater. Trans. JIM **42** (2001) 484-490.
9) M. Palm, G. Sauthoff, Intermetallics **12** (2004) 13451359.
10) M. Palm, J. Lacaze, Intermetallics **14** (2006) 1291-1303.
11) G. Ghosh, in: G. Effenberg (Ed.), Ternary Alloy Systems, Springer, Berlin, 2005, pp. 426-452.
12) P.R. Swann, W.R. Duff, R.M. Fisher, Metall. Trans. **3** (1972) 409-419.
13) S.M. Allen, J.W. Cahn, Acta Metall. **24** (1976) 425-436.
14) C.W. Su, C.G. Chao and T.F. Liu: Scr. Mater. **57** (2007) 917-920.